ANNUAL REVIEWS

Annual Review of Physical Chemistry

Spectroscopy and Scattering Studies Using Interpolated Ab Initio Potentials

Ernesto Quintas-Sánchez and Richard Dawes

Department of Chemistry, Missouri University of Science and Technology, Rolla, Missouri 65409, USA; email: dawesr@mst.edu

Annu. Rev. Phys. Chem. 2021. 72:399–421

First published as a Review in Advance on January 27, 2021

The *Annual Review of Physical Chemistry* is online at physchem.annualreviews.org

https://doi.org/10.1146/annurev-physchem-090519-051837

Keywords

potential energy surface, electronic structure theory, quantum dynamics, rovibrational spectroscopy, scattering

Abstract

The Born–Oppenheimer potential energy surface (PES) has come a long way since its introduction in the 1920s, both conceptually and in predictive power for practical applications. Nevertheless, nearly 100 years later—despite astonishing advances in computational power—the state-of-the-art first-principles prediction of observables related to spectroscopy and scattering dynamics is surprisingly limited. For example, the water dimer, $(H_2O)_2$, with only six nuclei and 20 electrons, still presents a formidable challenge for full-dimensional variational calculations of bound states and is considered out of reach for rigorous scattering calculations. The extremely poor scaling of the most rigorous quantum methods is fundamental; however, recent progress in development of approximate methodologies has opened the door to fairly routine high-quality predictions, unthinkable 20 years ago. In this review, in relation to the workflow of spectroscopy and/or scattering studies, we summarize progress and challenges in the component areas of electronic structure calculations, PES fitting, and quantum dynamical calculations.

1. INTRODUCTION

PES: potential energy surface

Since its introduction in the 1920s, the Born–Oppenheimer approximation (1), which separates the molecular Hamiltonian into electronic and nuclear parts, has provided a framework with which to understand molecular systems on qualitative and quantitative levels. Qualitatively, the consequent molecular potential energy surface (PES) serves as a model that to a familiar viewer illustrates the structural isomers of a system, their relative energies, their flexibility or floppiness, and the feasibility of interconversion (**Figure 1**). The key role of barriers and bottlenecks on the PES guided the development of kinetic theories, such as the transition-state theories of the 1930s (2, 3). Quantitatively, the PES serves as a defining part of the Hamiltonian for the nuclei and can thus be used in a wide variety of calculations, ranging from bound or resonance rovibrational states (providing predictive insight into spectroscopic observables) to cross sections and rates of various collisional processes (elastic, inelastic, and reactive) and even—though usually involving multiple PESs—to simulations of the photophysics and photochemistry triggered by the absorption of energetic photons. Through the Born–Oppenheimer approximation, the electronic energy can be considered for any given fixed geometry of the nuclei. The electronic wave function describing a molecular system—and its energy—generally varies as a function of the relative positions of the nuclei; therefore, the PES becomes the function describing the electronic energy of the system, evolving as a function of its geometry. The various eigenstates of the electronic Hamiltonian correspond to the set of electronic states of the system, each represented by a PES, one or more of which may govern the states or dynamical processes of interest. A great deal of literature is available relating to the history and development of the PES concept (4, 5), its physical and mathematical properties

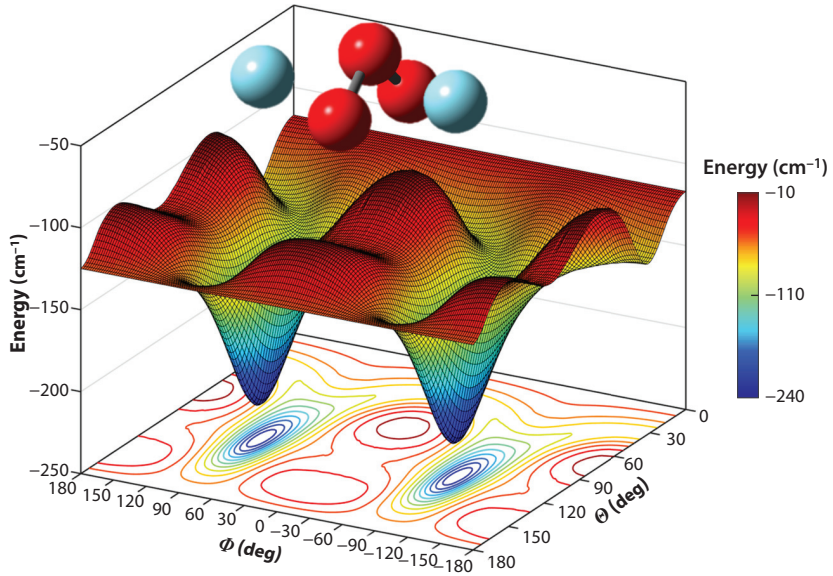

Figure 1

Two representations of a global potential energy surface (PES) describing O_3–Ar interactions. The surface-plot rendering provides a clear three-dimensional visualization of the general topography of the PES. The contour plot (projected at the base of the figure) provides a less visceral but more precise communication of the nature of the interactions, including the position of minima, transition states, and isomerization paths. Above the plot, two Ar atoms (*cyan*) show the symmetric positions of the global minima, on opposite faces of the O_3 molecule (*red*).

and constraints (such as symmetries and behavior at long range) (6), and its subtle and not so subtle extensions, introducing so-called non-Born–Oppenheimer corrections or couplings (7).

In this review, we focus on the components of the workflow of a computational spectroscopy or scattering study—that is, what electronic structure methods or model chemistries are suitable for the production of electronic energies of sufficient accuracy, whether or how to fit them into a usable PES or PESs, and how to employ them in calculations of the spectroscopic or dynamical observables of interest. Note that it is always an option to bypass PES construction entirely and simply compute all the necessary quantities, as needed, on the fly. This option may be enticing if the fitting procedure for a given system is particularly challenging, but it is very costly if high-level data are required and thus is best suited for applications where trajectories at a modest level of theory are applicable. The nature of the system under study and the dynamical quantities of interest, in turn, dictate the challenges and requirements relating to the preceding steps in the workflow. For example, if one plans to study inelastic collisions (collisional energy transfer) between two nonreactive closed-shell species, then the requirements for the coordinate and energy ranges of the PES—as well as the underlying electronic structure approach—will all be very different than for a study of reactive collisions, which may involve bonding rearrangements and drastic changes in the electronic structure of the system. Similarly, a study of rovibrational states that are strongly confined to the region of a single well permits different methodologies than those required to study floppy, multiwelled systems, fraught with delocalization and tunneling.

CC: coupled-cluster

AI: artificial intelligence

The two dynamically very different example cases of (*a*) inelastic collisions between two nonreactive closed-shell species and (*b*) rovibrational states that are strongly confined to the region of a single well are likely to be similar in terms of the most suitable and affordable high-accuracy electronic structure approach. In the absence of exotic multiconfigurational electronic structures, and depending on the number of electrons, both cases are typically amenable to a single-reference-based [e.g., coupled-cluster (CC)] protocol. In contrast, from a PES construction and fitting standpoint, those two cases could differ greatly in the type and range of relevant coordinates. Inelastic scattering predictions can be very sensitive to subtleties of the long-range behavior of the PES, while low-lying spectroscopic levels may be very sensitive to the precise shape of the PES only in the region of a strongly confined well.

Similarly, the other two cases mentioned above—reactive collisions and the spectroscopy of floppy, multiwelled systems—may share similarities in the necessary electronic structure approach, perhaps requiring a multireference method to handle the changes in electronic structure associated with bonding rearrangements or exploration of large regions of the configuration space. Here, corresponding challenges may arise in PES construction and representation, since the effectiveness and convenience of particular choices of coordinates and fitting functions may differ for wildly different geometries or product channels. In the example of proposed scattering calculations for the water dimer, $(H_2O)_2$, accurate electronic structure calculations are affordable, and accurate representation of the 12-dimensional PES is also achievable (8); only the scattering calculations are prohibitively expensive. In contrast, until recently the accuracy of scattering calculations for the three-atom system $O_2 + O$ (9–11) was limited by challenges in the electronic structure calculations (12, 13), related to the important effects of strong (static) and dynamic electron correlation and perturbations from excited electronic states (14).

The goal of this review is to cover some of the available and emerging high-accuracy electronic structure methods applicable to systems with up to roughly 12 nuclei and 100 electrons (those accessible to rigorous quantum dynamical treatment). We also cover methods and trends in the area of PES construction and representation. Finally, we highlight a variety of traditional as well as new avenues for computing spectroscopic and dynamical quantities. A theme connecting all of these areas is that of automation and artificial intelligence (AI). Parallel high-performance computing

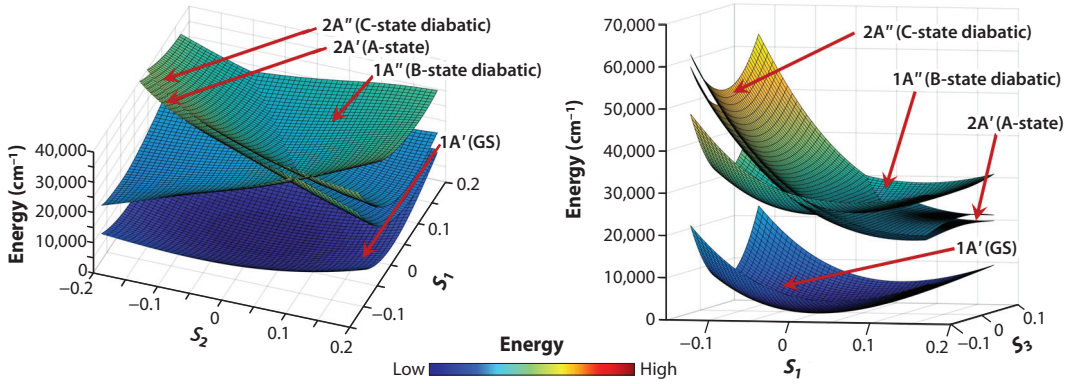

Figure 2

The four lowest electronic states of NO_2 are plotted as a function of pairs of normal-mode coordinates (S_1 and S_2 at left, and S_1 and S_3 at right). We computed the energies at the MRCI-F12 level. The two coupled states of A″ symmetry (the B and C states) intersect in the Franck–Condon region and are shown in a diabatic representation. Abbreviations: GS, ground state; MRCI, multireference configuration interaction; S_1, symmetric stretch; S_2, bend; S_3, asymmetric stretch.

and machine learning (ML) are transforming how we do science. Scripting of multicomponent electronic structure protocols is becoming commonplace. Methods using AI to adapt and tailor those procedures are emerging. Similarly, automated PES construction and the use of ML to provide PES models are a rapidly developing field. In the area of computational spectroscopy, not only have there been breakthroughs in eigensolvers and linear algebra, but also automation is being applied for spectroscopic databases, where the generation and curation of lists of transitions (sometimes billions of lines for a single species) are necessarily systematized.

2. THE CONSTRUCTION OF AB INITIO–BASED POTENTIAL ENERGY SURFACES

Given the central role of the PES in determining the states and behavior of molecular systems, many approaches to its construction—varying in sophistication—have been employed. Beginning in the 1930s, empirical and semiempirical procedures were used to determine general features of the PES (15) and constrain and parameterize simple functions (16), and in some cases, physical models constructed from plaster (17) or plywood (18) were made. Although the early models were somewhat primitive, insightful analyses were already under way—such as Teller's (19) research on the crossing of PESs, which is still cited today. Asymptotic behavior (20) and analyses such as symmetry adapted perturbation theory (SAPT) (21–23) are powerful tools, but in modern usage they are guided by decades of advances in electronic structure theory that, combined with huge computing power, now permit us to benchmark the PES via accurate estimates of the electronic energy at arbitrary locations. In systems where the Born–Oppenheimer approximation either breaks down entirely or is not sufficiently accurate, it can be necessary to construct multiple coupled PESs (**Figure 2**). Such PESs can be used to explore nonadiabatic dynamics, including photodissociation (24), as well as to study states and processes in which perturbations, coupling mechanisms, and geometric phase effects are relevant. Electronic structure calculations yield energies in the adiabatic representation and, thus, in the region of state intersections will exhibit cusps (derivative discontinuities) that are problematic for fitting strategies. While this is an active area of development, most approaches to nonadiabatic dynamics prefer a diabatic representation

ML: machine learning

SAPT: symmetry adapted perturbation theory

of the PESs, in which states tend to be smooth, with slowly varying character, retaining their identity as they cross one another. Coupled to one another in this representation, the PESs become a potential energy matrix, with each off-diagonal term representing a geometry-dependent surface of the coupling between the states connected by that element (7, 25). These areas are the frontier of small-molecule quantum dynamics. For small-enough systems, arbitrarily accurate results can be produced within the Born–Oppenheimer approximation. For larger systems, high accuracy is still a challenge, and affordable methods such as density functional theory are very actively under development. For the largest systems, such as proteins, parameterized models (force fields) are still the most common approach. Here, we focus on wave-function-based ab initio methods, which, although limited by steep cost scaling, provide a systematically improvable framework with which to obtain highly accurate PES data.

HF: Hartree–Fock

CBS: complete basis set

FCI: full configuration interaction

2.1. Ab Initio Calculations

Ab initio electronic structure calculations are used to produce accurate values of the PES at particular molecular geometries. Due to the relatively high cost of each such calculation in high-accuracy applications, ab initio energies are rarely used directly in dynamics calculations, which can require up to millions or even billions of PES evaluations. Rather, the number of ab initio data points is usually limited to the minimum needed for accurate representation of the global PES through a fitting approach. Thus, typically a few thousand ab initio data points are fitted into an analytic PES that can be efficiently evaluated as needed. The electronic structure calculations themselves are certainly the most accessible part of the overall workflow, as many packages—both commercial and academic—are available (26–32). Wave-function-based ab initio quantum chemistry methods solve the electronic Schrödinger equation given only the total number of electrons and the positions of the nuclei in the system, with (for nonrelativistic calculations) no other hypotheses than the following: (*a*) Coulomb forces are the only ones defining the interactions between all electrons and nuclei, and (*b*) the electrons obey Fermi statistics and the Pauli exclusion principle, that is, without appealing to experiments, beyond invoking the numerical values of fundamental physical constants.

In traditional nonrelativistic wave-function-based theory, there are essentially two classes of approximations to be considered. The first approximation is related to the (one-electron) basis functions to be used in the molecular orbital (MO) representation. The second concerns the expansion of the electronic wave function. In most cases, Gaussian basis functions are used to approximate the MOs—since computing the required integrals can be accomplished efficiently using this basis—while the many-electron wave function is typically represented as antisymmetrized products (Slater determinants) of the MOs. The two are related, since larger basis sets permit construction of additional orbitals, which can potentially be included in a more complete wave-function expansion. In the simple example of a single Hartree–Fock (HF) determinant, the additional basis functions serve only to increase the flexibility of the one-electron MO description, tending asymptotically toward an infinite (complete) set of functions, known as the complete basis set (CBS) limit, and in this case the HF limit. In post-HF calculations, various means are employed to increase the flexibility and accuracy of the wave-function expansion. Ideally, in a full configuration interaction (FCI) calculation, every possible Slater determinant is used (i.e., all physically allowable electronic configurations are included in the calculation), which provides the most accurate result possible for the given one-electron basis set employed.

2.1.1. Single-reference and multireference methods. Conventional ab initio approaches are often classified into two main groups: single-reference and multireference methods. This

MRCI: multireference configuration interaction

designation (single-reference versus multireference) simply indicates whether or not the electronic wave function is being represented (expanded from) by a single dominant configuration (Slater determinant). We have recently discussed the many considerations that go into planning a PES construction project in terms of selecting an appropriate single- or multireference method or protocol (33). Construction of a global PES can be much more demanding of the electronic structure methods than analysis of only a few critical points such as minima and asymptotes. Not only does one seek a balance in terms of the highest possible (or necessary) accuracy with manageable computational costs, but also, if a high-fidelity fit is desired, one requires a consistent and robustly converged data set across the entire coordinate space relevant to the application. Determining an accurate and well-behaved protocol is perhaps the most challenging and important step in the overall process, since fitting methods—especially interpolative ones—are typically not designed to accommodate irregularities, and even minor spurious topographies could affect the results. As discussed in Reference 33, the applicable methods depend strongly on the nature and dynamics of the system of interest. Whenever possible, for small to medium-sized systems, the method of choice for PES construction is the size-consistent and size-extensive CC method, specifically, the gold-standard CCSD(T) method. It is fair to say that when CCSD(T) is not used, it is usually because it is not applicable [e.g., because of related issues such as the state of interest being an excited state of the given symmetry and spin, strong multireference character, convergence problems in CCSD(T) itself or in the HF reference] or, rarely, not sufficiently accurate. The ultimate goal is to capture the strong (static) and dynamic electron correlation as accurately and cost-efficiently as possible. Common implementations of CCSD(T) are known to scale in cost as n^7 with the number of electrons, and costs rise steeply through the correlation treatment hierarchy, reaching n^{10} at CCSDTQ. Going beyond CCSD(T) in systems that are well described by a single determinant is rather uncommon but is sometimes observed in high-accuracy applications (34–36). At present, high-order CC implementations are not as robust as those up to CCSD(T), nor are they as widely available. There is, however, considerable development effort devoted to CC theory. Some efforts address the cost/accuracy issues either through new algorithms or representations (37–39) or by introducing various types of approximations (40, 41). When CC fails to either converge or accurately describe the system, one often turns to multireference methods such as multireference configuration interaction (MRCI). MRCI is the most common approach for systems with strong multireference character such as ozone, as well as for excited states, or multistate PESs (42). MRCI is neither size consistent nor size extensive, and it often requires considerable experience to specify crucial details such as the choice of active space. MRCI is also very expensive even at the standard level of single and double excitations, and no affordable rigorous treatments of high-order correlation are available. Often, a posteriori corrections related to those proposed by Davidson & Silver (43) are added, aiming to improve size consistency and extensivity, and thus to implicitly account for some of the missing high-order correlation. These corrections often improve accuracy but can introduce nonphysical behavior and numerical issues that impair the process of fitting a PES (33). Aside from all that, it's fantastic! A realistic perspective is that it is not so much that MRCI suffers so many drawbacks, but rather that the cases for which it is warranted are extremely challenging. Furthermore, many of the cases where a multireference approach might be indicated, such as a reactive PES describing fragmentation of a molecule and large changes in the electronic structure, will also involve multiple electronic states (either becoming degenerate in some region or asymptote or exhibiting dynamically relevant crossings or avoided crossings). When constructing a PES, it can be necessary to consider a balanced multistate electronic structure treatment simply to obtain the correct behavior for a single state of interest (33).

Considerable effort in electronic structure method development continues to be expended on the strong correlation problem and on recovering the desirable properties of the CC approach in

these applications. Various multireference extensions and modifications of CC have been or are being tested (41, 44–47), along with other approaches, such as Monte Carlo–based methods (48, 49), the density matrix renormalization group (50, 51), Green's function methods (52, 53), and so forth. For excited states, various equation-of-motion CC methods have been introduced (48, 54, 55). So far, however, in the construction of PESs based on multireference ab initio data, the use of methods other than MRCI (or lower-level methods such as CASSCF or CASPT2) is quite rare. This is mainly because construction of a PES typically involves generating thousands of data points, which favors mature robust methods that are implemented in available software packages. Ideally, for automated PES construction, data can be reliably generated and extracted via scripts.

2.1.2. Compound methods or protocols. Given the steep cost scaling of converging electronic structure calculations (in both directions, basis set completeness and correlation treatment) toward the FCI/CBS limit, a practical approach is to adopt a composite scheme. Various schemes have been introduced. Generally, the idea is to converge as well as possible the total energy while limiting costs by splitting the calculation into several independent contributions, balancing the effort applied to each term on the basis of its significance and cost scaling. For example, in a single-reference CC-based application, one might separate the correlation treatment hierarchy by order, and thus attempt to converge the CCSD contribution using very large (or extrapolated) basis sets, and then estimate as many of the higher-order contributions—(T), T, (Q), Q, and so on—as are deemed necessary, using sequentially smaller basis sets to balance the rapidly exploding costs with the hopefully rapidly decreasing significance of each term. Using explicitly correlated methods [e.g., CCSD(T)-F12, or MRCI-F12] is a popular way to accelerate basis set convergence at a given correlation treatment level (56), although doing so involves introducing approximations and numerical machinery that some researchers prefer to avoid, relying instead on standard extrapolation toward what should in principle be the same CBS limit (57, 58). Most high-accuracy schemes take a holistic view of the contributions and might separately evaluate valence and core electron correlation, high-order correlation, relativistic corrections (including spin-orbit effects), and perhaps non-Born-Oppenheimer corrections (e.g., the diagonal correction) (59, 60).

2.2. Fitting Methods

Many PES-fitting methodologies have been proposed or are in active development. Traditionally, the push was toward new strategies to fit the calculated energies more efficiently, with higher accuracy and more systematic control over fitting errors. At present, more effort is being directed toward developing black-box (e.g., ML-based) models that are less system specific and lend themselves to automation. Most PES-fitting strategies can be broadly categorized—although the borders of the classifications are sometimes blurry—according to two different criteria: (*a*) whether a physical or a more mathematical representation is employed and (*b*) whether the fit is interpolative or not. One may further distinguish between methods that use linear versus nonlinear algebra to determine model parameters.

With regard to the set of functions employed in the fit, these models can be classified as physical or mathematical methods; the physical approaches are typically more intuitive (less black-box) and are based on fitting using a physically motivated set of functions. With physical methods, the functional form is usually derived by taking into account as much information about the system as possible (such as symmetry and asymptotic behavior); if the functions are chosen appropriately, the PES representation can be accurate, require a minimal quantity of fitting data (especially in the long range), be compact (with a minimal number of fitting parameters), and be efficient to

GP: Gaussian process

NNs: neural networks

IMLS: interpolating moving least squares

evaluate. The main drawback is that the procedural details are very system specific. An example of such fitting approaches is the Morse/long-range method by LeRoy and colleagues (20, 61–63), which builds the precise long-range behavior of the specific system into the fitting functions. The representation of the long-range interaction between molecules or fragments (very relevant for low-temperature scattering studies) is well described as a function of multipole expansions. Within this formulation, the necessary parameters defining the interaction potential correspond directly to physical properties of the interacting fragments (such as multipole coefficients and polarizabilities). The multipole formalism has been developed over decades (64), and there are still some efforts to develop related approaches, such as distributed multipoles (65). At sufficiently long range, it is hard to beat the multipole expression for describing the PES. Indeed, in our tests, high-level ab initio calculations performed in the long range can often be reproduced to within 0.001 cm^{-1} by only a few simple terms.

SAPT is another sophisticated physically based framework for computing noncovalent interactions that also enables analysis in terms of decomposition of the energy into contributions such as electrostatic, exchange, induction, and dispersion (21–23). Based on perturbation theory, various levels of SAPT are designated by order of truncation of the expansion. Current development efforts in SAPT aim to improve accuracy, as well as to treat open-shell systems, degeneracies, and excited electronic states (66, 67). However, in terms of global PESs, these methods are simply not applicable at short distances (LeRoy and colleagues' consideration of the nuclear coalescence extreme notwithstanding); therefore, a common strategy is to switch from using some other approach at short distances to using a physical analytic description of the system's interactions at long range (13).

In contrast, in a more mathematical approach, the chosen functional form typically does not strongly enforce assumptions concerning the physical nature of interactions in the system but rather depends more on its efficiency and flexibility. Many different types of functions have been used, including (but not limited to) polynomials, sigmoid-like functions, splines, Gaussians, and Morse functions. The aim of a mathematical approach is to fit—as accurately as possible—a set of data points to an analytic expression constructed with a combination of extremely flexible functions (usually without any direct physical meaning). Some examples of mathematical methods include spline methods (68), interpolating moving least squares (IMLS) (69–71), modified Shepard interpolation (72), reproducing kernel Hilbert space (73), Gaussian process (GP) regression (74–76), neural networks (NNs) (77–79), genetic algorithms (80), and the permutationally invariant polynomial (PIP) method (81). Hybrid approaches such as PIP-NN (82), fundamental invariant NN (83), and PIP-IMLS (84, 85) illustrate that elegant features of one method—such as the treatment of symmetry in the PIP approach—can be introduced into the framework of another methodology. Within the realm of mathematical methods, there can still be important differences in terms of how far removed the method is from a clearly understood physical model. For example, if one fits a data set using a fixed basis of Morse (or other similar) functions, and uses linear algebra to obtain a set of model coefficients, then it is still quite intuitive what is going on, and such a well-defined approach will (repeatably) lead to a particular set of fitting coefficients. Indeed, functions such as Morse are chosen because they retain some physical aspects, such as becoming slowly varying at long range. In this context, one could adjust the number (or weighting) of data points in a given region, and—within the flexibility of the fitting basis—expect corresponding changes to the fit in that region. ML-based approaches (86) such as NNs are rapidly gaining popularity but are much more obscure, usually employing activation functions with no resemblance to PESs. Furthermore, such nonlinear approaches are not deterministic in the same way as those based on linear algebra, and different solutions are obtained each time the fitting procedure is executed. NN methods can be guided by data density and placement, as well as by choices such

as the number of neurons and hidden layers, but can still be difficult to systematically control toward a specific (especially high) accuracy target. Proponents of ML methods see great potential in removing human intuition from the procedure and letting AI identify hidden correlations to improve the model representation (87). Of course, it is still advantageous and even necessary to correctly account for things like permutation symmetry and translational invariance, and these properties have recently been successfully enforced in some ML models (86). There is no doubt that ML methods are an exciting area of research and development that hold great promise to broadly redefine computational chemistry, and thus can be expected to become ever more popular. Done carefully, a mathematical approach to fitting can result in a PES that is numerically accurate and computationally efficient. An advantage of this kind of less-constrained fitting is that an accurate PES can be constructed even for cases with unusual topographies, although special care must be taken during the construction process to ensure an asymptotically and globally correct physical shape, avoiding the presence of holes or other spurious behaviors due to the use of nonphysically motivated—or excessively flexible—functional forms. A highly successful approach to describing water–water interactions ranging from the dimer to the bulk, and recently including solvated ions, is the MB-pol approach of Paesani and colleagues (8). MB-pol can be described as a hybrid of many of the abovementioned strategies. It is based on high-level ab initio calculations and in the short range employs ML methods to determine flexible model parameters while also incorporating a physically motivated form for the long range; thus, overall it relies on switching and damping, with both linear and nonlinear parameters (8).

PES-fitting methods can also be classified as interpolative or noninterpolative. An interpolative fit passes exactly—or arbitrarily nearly so—through each data point, making the fitting error negligible near data points. In contrast, noninterpolative fits may or may not pass through any of the individual data points, but rather accommodate all of them in a balanced (often a least-squares) way. In general, modern interpolative fitting strategies can in principle satisfy any accuracy target (precision of the PES) and, if necessary or desired, can be further improved or optimized in any particular region of the PES by simply adding more ab initio data points. However, early implementations of interpolative methods, such as cubic splines, suffer from serious limitations, remnants of which are still relevant to more modern methods. Cubic splines, although very straightforward to implement, generally require a dense regular product grid of data, making them among the least efficient PES representations in terms of the number of required electronic structure calculations (68). They are also notorious for exhibiting spurious oscillations in regions where the density (though presumably already quite high) is still not sufficient. For cubic splines, due to the regular product structure of the data grid, improving the fit in even a small region may require adding a considerable quantity of data globally, or redefining the grid altogether. Modern interpolative methods can handle arbitrarily irregular data sets with greatly varying density. This means that the fit can be adjusted in a particular region by the addition of only a single data point. Remarkably, given the very poor efficiency of the cubic splines method, the newest methods are perhaps the most efficient in terms of reaching high fitting accuracy with limited ab initio data (75, 88). Nevertheless, a concern even for modern interpolative methods is that of possible oscillations in regions with insufficient data coverage, or wild divergencies where data coverage is lacking entirely. These behaviors are possible with any mathematical approach but can be exacerbated in interpolative methods because of the common use of highly peaked weight functions that make the fit less constrained by global behavior. In our research into interpolative fitting methods, we find that these undesirable behaviors can be largely avoided by using physically motivated functions to perform the interpolation, as well as by linear algebra techniques such as limiting poor conditioning of the design matrix through a procedure that we refer to as dynamic conditioning. This procedure has been described elsewhere (88) and uses the singular value decomposition

method to identify and employ only the best-determined linear combinations of the fitting basis, and since individual fits are quite localized, the basis is effectively dynamically tuned across the varying topography of the global PES.

RMSE: root-mean-squared error

L-IMLS: local IMLS

There are relatively few direct comparisons between fitting methods, but a recent comparative test found that PIP, NN, and Gaussian approximation potentials performed similarly in fitting two-body MB-pol energies [root-mean-squared error (RMSE) of ∼0.05 kcal mol^{-1}] (76). In a comparison between NN and GP regression, where both methods employed identical fitting points to fit a PES for formaldehyde and then tested for statistical accuracy as well as performance in vibrational calculations, both methods achieved similar sub-wave-number fitting error using 2,500 data points, but GP was significantly more accurate (especially in the computed spectrum) when smaller data sets were used (89). Generally, each method has its own performance characteristics in terms of implementation and use. Some factors that one might consider when selecting a method for a given application are (*a*) ease of use; (*b*) limiting accuracy and/or efficiency in terms of the quantity of data required to reach the desired accuracy target; (*c*) ability to precisely capture symmetry and/or key features of the topography such as the shape of wells, barriers, or the long range; and (*d*) efficient output in the form most useful to the spectroscopy/dynamics method. With these considerations in mind, the preferred method for a quasi-classical trajectories study of the isomerization of a large molecule, for example, would likely be different than that for a low-temperature quantum scattering calculation. Studies of spectroscopy and scattering dynamics place stringent demands on the PES. The results can be very sensitive to the fitting accuracy, the precise form of the long-range behavior, and a precise reflection of symmetry. For a variational calculation of rovibrational levels, one might place higher priority on fitting accuracy over the efficiency of PES evaluations, since the grid would likely be computed only once, at the beginning of a large set of calculations, and it is desirable to be able to interpret the results as a direct reflection of the underlying electronic structure method.

A method that we have employed and that lends itself to high-accuracy applications is IMLS. IMLS-based approaches are interpolative fitting methods, and thus exhibit high fidelity to the ab initio data set used in the fit and are systematically improvable by adding more data points. The efficiency of IMLS-based methods for constructing PESs with sub-wave-number fitting errors has been demonstrated (90–92), and general descriptions of its methodology—as well as various avenues of its development—are available in the literature (69, 70, 88).

Although high-degree IMLS fits are much less computationally expensive than high-level electronic structure calculations, their computational cost can still be high—relative to other fitting methods—since by default a weighted least-squares fit needs to be performed each time the PES is evaluated. The so-called local IMLS approach (L-IMLS) (71, 91) is a version of the IMLS method that stores local approximants to overcome this problem, retaining the features of an IMLS fit yet being much more efficient to evaluate. Roughly speaking, by using a single processor one might expect to make two to three thousand calls per second from an L-IMLS fit to a few thousand data points. This is two to three orders of magnitude faster than the parent IMLS method, for which one must set up and solve the design matrix during each evaluation. Note, however, that even the L-IMLS method is at least an order of magnitude slower to evaluate than, for example, a simple single-polynomial expansion. Of course, any fitting method is expected to be many orders of magnitude faster than direct computation of high-level electronic structure data, which can take between minutes and days per point. The main idea behind the L-IMLS methodology is that local approximants—each fitting a small neighborhood of ab initio data—are computed and stored, and then the interpolated energy is obtained as a weighted sum of the local approximants. More generally, a local approximant (or local fit) of the PES, for a given geometry **R** in the neighborhood

of the data point $\mathbf{R}_k$, can be defined as

$$v_k(\mathbf{R}) = \sum_{j=1}^{m} a_{j,k}(\mathbf{R}_k)\, B_j(\mathbf{R}), \qquad 1.$$

vdW: van der Waals

where m is the total number of basis functions $\{B_j(\mathbf{R})\}$ and the coefficients $\{a_{j,k}\}$ are determined using a standard IMLS fit. Then, given N local approximants $v_k(\mathbf{R})$, where $k = 1, 2, \ldots, N$, the L-IMLS potential at any given nuclear configuration (geometry) is defined as the normalized weighted sum of the local fits:

$$V_{\text{fit}}(\mathbf{R}) = \sum_{k=1}^{N} w_k(\mathbf{R})\, v_k(\mathbf{R}) \Big/ \sum_{k=1}^{N} w_k(\mathbf{R}), \qquad 2.$$

where $w_k(\mathbf{R})$ is the interpolating weight function. This way, a maximum of N weighted least-squares fits need to be done—only once—and a PES evaluation involves only a summation over the previously determined coefficients. Since the local fits for $v_k(\mathbf{R})$ are constructed and stored in advance, the method is much more efficient than the traditional IMLS implementation. Note that, although the total potential is globally accurate, each of the local expansions $v_k(\mathbf{R})$ is constrained only close to $\mathbf{R}_k$. This contributes to the accuracy of the method, since the full flexibility of the basis can be applied to only a small region, and each neighboring expansion can have different coefficients. A spectroscopic application to the $(NNO)_2$ van der Waals (vdW) system (91) found that, by use of local expansions of the angular basis, each truncated at sixth order, it was possible to match an equivalent single expansion of forty-first order (composed of more than 300,000 functions).

2.3. Automated Construction of Potential Energy Surfaces

All of the preceding discussion focuses on—for a given application—the importance of selecting an appropriate electronic structure method and a PES fitting strategy that will be used to provide an accurate and efficient representation. However, a crucial aspect of the process is the selection of the set of geometries at which to compute data (the total number of points and their locations). Some primitive methods such as cubic splines demand a product grid, discretizing and combining the maximum ranges of each coordinate into a vast hypercube. This process is very inefficient because it places data at dynamically inaccessible locations. In fact, even in six dimensions, corresponding to the PES of a four-atom system, the dynamically relevant region becomes a small fraction of the total product of coordinate ranges. This has been well known for a long time, and most efforts to construct PESs employ some strategy to select point locations more efficiently, confining them to relevant accessible locations. Running trajectories is a popular approach, although one may have to be generous with the energy in order to allow for tunneling and also ensure that disconnected regions are found. It can also be problematic for the fitting representation if the fitting data are carefully restricted but then the functions used to perform, for example, a vibrational calculation, perhaps less well confined, find holes in the PES. Efficient means to locate and patch holes have been developed for this reason (93).

Various data-placement strategies, including random, low-discrepancy sequences such as Sobol, regular grids, distributions along reaction paths, or any combination thereof (perhaps biased by energy or other importance determinations), have been implemented. What is less clear in the pursuit of efficient PES representation—that is, achieving accuracy targets while using the fewest possible points—is whether there is an optimal distribution of points for a given number of points and a given fitting method. Indeed, in the comparison between NN and GP fitting for the

spectroscopic application mentioned above (89), it is not obvious that the shared data sets were optimal for both fitting methods. Some methods provide a local measure of fitting uncertainty and thus lend themselves to systematic refinement (74, 75, 88). This can be done automatically and can not only target the fitting accuracy but also directly target the convergence of dynamical quantities computed with the PES. Note that targeting a global fitting accuracy measure might not be the most efficient way to refine a PES for a given application. For example, in a vdW system, reaching 1 cm^{-1} RMSE in the region of a well or wells might sufficiently converge calculations of rovibrational bound states. In contrast, for a low-temperature scattering study, sensitivity to the long-range part of the PES will typically demand much better than 1 cm^{-1} accuracy (a huge relative error) in that region but will be less sensitive to the accuracy in the close-interaction region. Automated PES construction, including the generation and fitting of data as well as subsequent refinement toward user-specified targets, is certainly the way of the future and, to an already impressive degree, the way of the present (87, 94–96).

In our own research, we have developed a family of software codes named AUTOSURF (94) that make efficient use of large-scale parallelization and completely automate the PES construction process, generating and fitting ab initio data, by interfacing to popular electronic structure codes. Tailored to high-accuracy applications in spectroscopy and scattering dynamics, AUTOSURF is tuned to reach an RMSE of $\sim$1 cm^{-1} or lower. The fitting algorithms implemented in the code are based on the L-IMLS methodology and have been under development for several years; L-IMLS potentials based on this approach have been constructed for numerous systems (13, 42, 85, 91, 92, 97–101). PES construction begins with a sparse distribution of ab initio data placed either randomly or according to a Sobol sampling sequence; then a local error-estimation scheme determines where new data are required and, in a series of iterations, computes new ab initio data and updates the fitted PES until a specified accuracy is reached. The ultimate goal is to represent the ab initio data with such high fidelity that, when used in theoretical dynamics and/or spectroscopic studies, the results directly reflect the underlying level of the electronic structure method.

3. SPECTROSCOPY STUDIES

Computation has solidified its role as a full partner to experiments in describing the many types of light–matter interactions needed to predict, and interpret, the wide variety of spectroscopic techniques that have been developed over more than a century. The complete simulation of an absorption spectroscopy experiment, for example, requires not only computing the relevant initial and final states but also obtaining the intensities of the radiative transitions between such states as governed by dipole or other mechanisms; therefore, one also requires the corresponding property surface(s), which can similarly be constructed by fitting ab initio data. Additional calculations or models might be applied to estimate line widths and shapes. Understanding radiative processes in the Earth's atmosphere (as well as others) helps us appreciate the effects of trace gases on our environment and climate. Studies in interstellar and circumstellar space have provided great insight into the history and evolution of the Universe. Confirming the presence and role of different species throughout space informs our models and strongly influences our understanding of the mechanisms of chemical networks and rates of star formation, as well as the composition, age, and origin of particular regions and structures. Radiative and detailed state-to-state collisional processes are key aspects of energy flow in low-density gases, where the collision frequency is low and local thermodynamic equilibrium is not observed. Molecular spectroscopic databases—such as HITRAN (105)—compile high-resolution lists of the transitions (sometimes billions) associated with each of hundreds of species, in addition to documenting intensities, line-shape parameters, and even collision-induced absorption data sets.

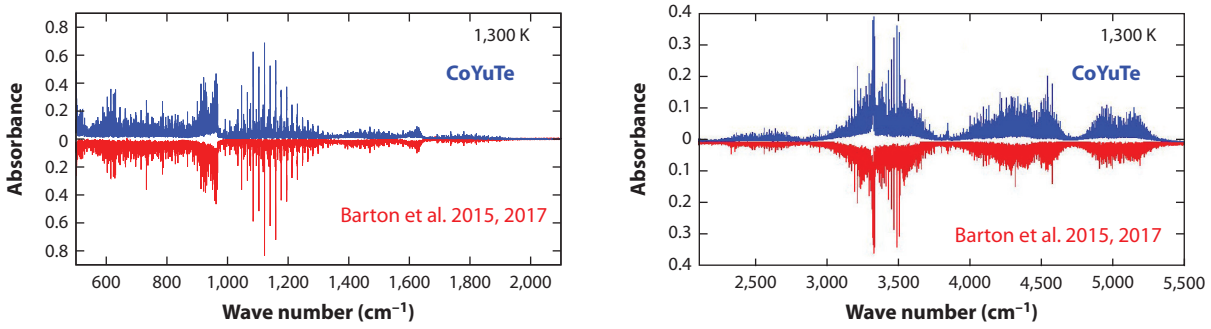

Figure 3

Comparison of a synthetic absorption spectrum for NH_3 [computed using CoYuTe, a comprehensive list of NH_3 spectroscopic transitions constructed as part of the ExoMol project (108)] with measurements by Barton et al. (102–104) at a temperature of 1,300 K. Figure adapted from Reference 108 with permission under a Creative Commons Attribution License (CC BY 4.0).

Although the contribution of computational spectroscopy to such databases is rapidly increasing, complete first-principles predictions of the positions, intensities, and line shapes of high-resolution spectra are rare. This is because the precision of predicted rovibrational spectra in terms of the line positions—even for small molecules—is limited to, at best, ~0.01 cm^{-1}, more commonly 1–5 cm^{-1}, and not uncommonly up to 40 cm^{-1} (106), depending on the system; in contrast, experimental data are often obtained with a precision of 0.001 cm^{-1} or better (107). Moreover, calculated (absolute) intensities are often accurate to within only 10% or so, and certainly reaching 1% accuracy is a major challenge for any theoretical study. Nevertheless, computation is still a powerful tool in this context, since it makes it possible to understand states and their energy patterns. For this reason, semiempirical refinements can greatly aid in assigning and estimating positions of dark states (**Figure 3**) (108–110). More generally, outside of high-resolution spectroscopy, the number and character of bound states—and their density—can strongly influence the properties and dynamics of the system, as well as its thermochemistry. For these reasons, there has long been great interest in computing rovibrational states without necessarily considering radiative transitions or, at least, not their intensities or line shapes. Here, we focus mainly on calculations of rovibrational states and transitions using fitted ab initio PESs.

Local PES expansions such as a Hessian (second order) can be used to estimate the vibrational level structure of a molecule, assuming that the states are confined to the region of a single well. This type of so-called normal mode analysis makes severe approximations, so more sophisticated methods are required even for the estimation of thermochemical partition functions, which are not overly sensitive to line positions but rather to state densities. Higher-order extensions and various other approximations have been proposed, but here we discuss methods to numerically solve the rovibrational Hamiltonian as accurately as possible, with few or no approximations. A variational solution to the rovibrational Hamiltonian employing a numerically exact kinetic operator and a global PES permits one to compute—within the Born–Oppenheimer approximation and the accuracy of the PES—the complete set of bound states (42, 111). The most common approach is to construct and diagonalize a matrix representation of the nuclear Hamiltonian in a given basis set. Many such procedures have been introduced, most of which employ discrete-variable or finite basis representations. The challenge, and what typically distinguishes different approaches, is how to deal with the extremely poor scaling of the most straightforward direct-product-basis approach. If between 10 and 100 functions are needed to describe each coordinate, then—even without considering rotation—the basis for a four-atom vibrational problem (six

dimensions of displacement) constructed in direct-product form would be between 10^6 and 10^{12} in size (which implies up to 8,000 GB of computer memory). The state of the art, for systems that are not special cases with high symmetry and/or rigidity, is approximately six atoms (112–114). In addition to employing large-scale computing and advanced linear algebra techniques, most strategies focus on greatly reducing the basis size, which includes finding a more compact and efficient set of functions (requiring fewer per dimension) and/or various pruning or contraction schemes. The goal is generally to retain the convergence of the full basis set as closely as possible, while rendering the computational effort manageable. In a recent article on methods to compute rovibrational spectra for molecules with more than four atoms, Carrington (115) points out three limiting issues: (*a*) basis size, (*b*) solving large eigenvalue/vector problems, and (*c*) computing matrix elements of the potential operator. Some methods that overcome these challenges—to some extent—and show promise for extending the range of system size that can be accurately studied have been reported. These include imposing a convenient sum-of-product form on the Hamiltonian, Smolyak grid approaches, and collocation methods (116–119). Of course, computing a long list of energies is rarely useful; therefore, considerable effort has gone into developing methods to organize and analyze states, helping to make assignments and interpret spectra (110, 120–122). Interfacing a variational code based on a parallel, symmetry-adapted, Lanczos iterative solver with our automated PES construction approach (AUTOSURF) has enabled us to compute spectra for a wide variety of vdW systems—including $(OCS)_2$ (97), $(CO)_2$ (100), $(CO_2)_2$ (98), CO_2–CO (123), CO_2–CS_2 (92), CO–N_2 (124), $(NNO)_2$ (91), CO_2–HCCH (99), C_6H^-–H_2 and C_6H^-–He (101), C_6H–He (125), O_2–CO (126), O_3–Ar (127), and CS–Ar and SiS–Ar (128)—enabling exploration of the impact of factors such as different well depths, fragment mass combinations, floppy coordinates, multiple minima, tunneling paths, symmetry, and vibrationally excited monomers.

4. SCATTERING STUDIES

Quantum scattering calculations provide the framework to predict and interpret the most fundamental chemical event: the outcome of a single collision, whether elastic, inelastic, or reactive. The study of chemical kinetics, since the introduction of the Arrhenius equation in 1889, has yielded deeper and deeper insights into reaction mechanisms, as postulated mechanisms and their implications for measurable rates were tested, refined or discarded, further tested, and so forth, which in some cases required invoking complex cycles of intermediates that were difficult or impossible to confirm. In the past several decades, we have gone past looking only at averaged rates and into the realm of detailed dynamics. The development of crossed molecular beam scattering experiments with precise initial-state selection has led to experiments with exquisite control and previously unimaginable insights into reaction dynamics, including the sometimes counterintuitive role of mode-selective chemistry. As a simple example, as Levine (129) points out, it has been confirmed that single collisions between Br_2 and Cl_2 are not reactive, but rather that the second-order reaction to produce ClBr proceeds via a cycle of intermediates. On the theory side, calculations provide access where experiments prove difficult or impossible, yielding insight in terms of properties of the molecules or fragments, features of the relevant PESs, and in some cases the role of resonances or couplings. Detailed experimental results—including cross sections, rates, and vector correlations (130)—provide stringent tests of PESs and dynamical approximations due to their sensitivity. Well-determined experimental data permit benchmarking of high-level electronic structure calculations and PES construction methods, as well as dynamical theories. It is important to note that some experiments, especially those at low temperature, are difficult to perform and can include unforeseen sources of error. Theory has, in turn, provided sanity checks and motivated new measurements or analyses.

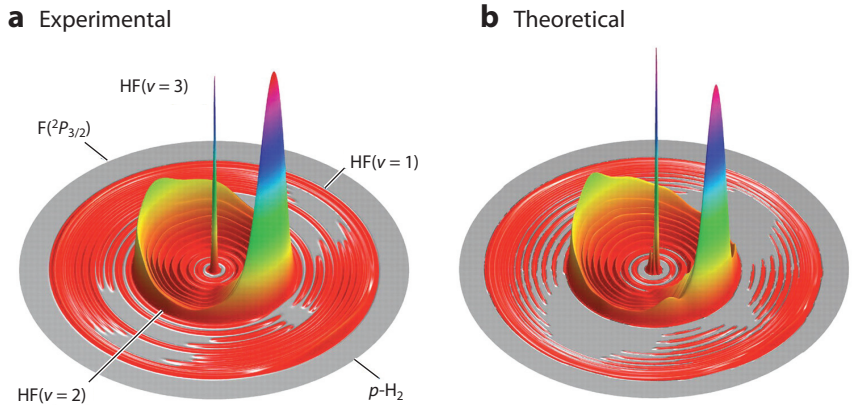

Figure 4

(*a*) Experimental and (*b*) theoretical three-dimensional contour plots for the HF product translational energy and angular distributions of the F + H_2 ($j = 0$) reaction. Different rings represent different HF rovibrational states. Figure adapted from Reference 135 with permission; copyright 2006 the American Association for the Advancement of Science.

Throughout their development, quantum scattering calculations have had a history of investigating astrophysically relevant systems. Much of the early research in this area was devoted to H + H_2 because of its relevance and relative simplicity, leading not only to methodologies that could be implemented numerically but also to a better understanding of issues relating to symmetry, as well as constraints for bosons and fermions (131). In fact, we are still learning the finer details of the H_3 system today (132). Reactive collisions between F + H_2, relevant to chemistry in the interstellar medium, have been extensively studied both experimentally and theoretically (133). As investigators sought to obtain higher accuracy and detailed features of the experiments on F + H_2, the system posed challenges for electronic structure calculations as well as for scattering theory. The HF reaction products, and their angular distributions, are governed by tunneling and are quite sensitive to the PES topology. The most precise low-temperature calculations demand an accurate treatment of nonadiabatic effects and the different spin-orbit levels of the F atom (134). The remarkable agreement between experiment and theory for this system (**Figure 4**) can be considered a triumph (135).

Currently, the feasibility of reactive scattering studies is limited by the poor scaling of rigorous fully quantum traditional methods. The most common traditional methods are based on time-dependent wave packets. A 2017 review (136) highlights impressive results for complicated reactions in systems with three or four heavy atoms, as well as more limited results for systems containing up to six atoms (but composed of mostly H atoms). Five- and six-atom systems are often treated in reduced dimensionality or through various approximations. At present, any such study—whether a comprehensive study of a three- or four-atom system or a more limited study of a five- or six-atom system—is a major computational effort that can take months, even using hundreds of computer cores, and assumes the availability of a prerequisite, suitably accurate PES (or PESs). PES construction for reactive systems is still a major challenge, since it can represent the toughest case possible for both the electronic structure method and the fitting approach. Bond breaking and formation often require the use of less black-box multireference methods, and frequently multiple (and different numbers of) electronic states will become degenerate at different product channel asymptotes, in addition to possible interactions and crossings of states

throughout the coordinate range of the PES. Constructing global PESs for multiple coupled electronic states requires special procedures such as diabatization and is at the frontier of both electronic structure theory and PES construction. Even a simplified description of the reaction of $O(^3P) + H_2$ involves at least four coupled PESs (137).

Nonreactive inelastic scattering is a much more approachable problem (138) in terms of both constructing a high-quality PES and treating the dynamics. Astrophysical applications are common, since in low-density regions—where local thermodynamic equilibrium is not observed and populations differ significantly from a Boltzmann distribution—detailed state-to-state calculations are needed to guide the theoretical models. The lack of reaction simplifies not only the electronic structure calculation but also the choice of coordinates, with no need to describe different initial and final states. The traditional rigorous approach to inelastic scattering dynamics is the time-independent close-coupling method, especially for low collision energies, although the use of time-dependent methods such as multiconfigurational time-dependent Hartree (MCTDH) is gaining popularity (139–141). Mixed quantum–classical methods have recently been improved and can drastically increase efficiency and thus the complexity of systems that are accessible (although with limitations due to classical approximations) (142). Historically, PES construction has been closely tied to the basis functions used in the dynamics. Large angular quadrature grids are computed at a series of radial separations (center-of-mass distances, R) of the fragments, then interpolated along R. This process is fairly demanding, since the strongly anisotropic close-interaction region could require a fairly high-order angular basis and, therefore, many ab initio data points. The L-IMLS method is particularly efficient at describing strongly anisotropic vdW interactions and has been successfully used in many applications (143–145). Automated PES construction facilitates studies of the differences between isomers or members of chemical families, where a series of PESs is needed. New experiments, and the corresponding calculations, are targeting the extremely cold regime, where low collision velocities can exaggerate quantum effects and place ever more stringent demands on PES accuracy. This is a signature area of the Nijmegen group; van de Meerakker and colleagues (146) have implemented various techniques used to slow (cool), control, and state-select different types of colliding molecules. **Figure 5** shows the remarkable agreement between measured and simulated scattering interference fringes.

5. OUTLOOK AND CONCLUDING REMARKS

It is an exciting time for both theoretical spectroscopy and dynamics, and the outlook for the near future is bright. Although the fundamental scaling of the most rigorous electronic structure and quantum dynamics methods remains prohibitively poor, through innovations in algorithms and the widespread use of high-performance computing, ML, and automation, we are entering a period of routine high-accuracy prediction, confirmation, and analysis/interpretation of experimental observables. The workflow of a computational spectroscopy or scattering project begins with selecting a suitably accurate electronic structure method, and then generating a data set that is sufficient to accurately determine a PES describing interactions in the relevant ranges of coordinate and energy. These steps have historically been huge bottlenecks, not only because of the amount of computing time required but also in terms of human time and expertise. Various high-accuracy electronic structure protocols are now available and can be reliably applied to different types of systems. Emerging electronic structure protocols will be self-tuning through AI, optimizing both accuracy and cost. The fundamental step of constructing a PES has historically been a tedious process conducted in system-specific ways by a few specialists. We are now seeing the release of more broadly usable PES-fitting methods that are largely automated, including the specification and generation of ab initio data sets. Finally, we are seeing breakthroughs in

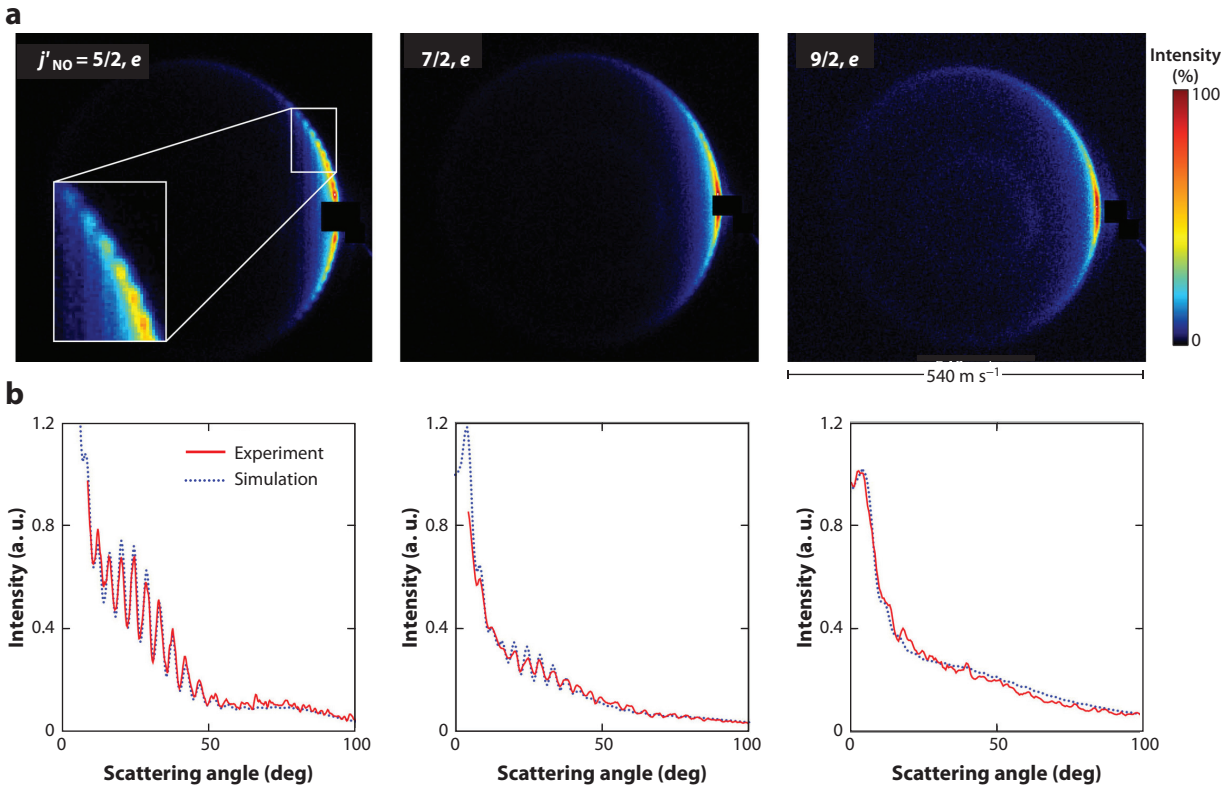

Figure 5

(*a*) Experimental images for the scattering processes NO($X^2\Pi_{3/2}, j_{NO} = 3/2, e + f$) + Ne → NO($X^2\Pi_{3/2}, j'_{NO}, e$) + Ne. (*b*) The experimental and simulated angular distributions. Figure adapted from Reference 146 with permission from AIP Publishing.

the capabilities and usability of variational spectroscopy and quantum dynamics codes. Efforts to benchmark and standardize rovibrational methods are under way, and interfaces to PES-fitting representations are enabling robust data management. In the area of quantum dynamics, better-scaling methods such as MCTDH are extending the range of systems that can be rigorously treated, and mixed quantum–classical approaches are extending them even further, albeit with some approximations. We are also seeing encouraging trends toward making codes—and research products such as PESs—freely available, as well as increasing participation through training both users and developers at workshops.

DISCLOSURE STATEMENT

The authors are not aware of any affiliations, memberships, funding, or financial holdings that might be perceived as affecting the objectivity of this review.

ACKNOWLEDGMENTS

The writing of this review was supported by the US Department of Energy (award DE-SC0019740) and the US National Science Foundation (grant CHE-1566246).

LITERATURE CITED

1. Born M, Oppenheimer R. 1927. Zur Quantentheorie der Molekeln. *Ann. Phys.* 389:457–84
2. Eyring H. 1935. The activated complex in chemical reactions. *J. Chem. Phys.* 3:107–15
3. Wigner E. 1938. The transition state method. *Trans. Faraday Soc.* 34:29–41
4. Schatz GC. 1989. The analytical representation of electronic potential energy surfaces. *Rev. Mod. Phys.* 61:669–88
5. Murrell JN, Carter S, Farantos SC, Huxley P, Varandas A. 1984. *Molecular Potential Energy Functions*. Chichester, UK: Wiley Intersci.

6. Presents an extensive and authoritative treatment of molecular symmetry.

6. **Bunker P, Jensen P. 2006. *Molecular Symmetry and Spectroscopy*. Ottawa, Can.: NRC Res.**
7. Domcke W, Yarkony D, Köppel H. 2011. *Conical Intersections: Theory, Computation and Experiment*. Adv. Ser. Phys. Chem. 17. Singapore: World Sci.
8. Babin V, Leforestier C, Paesani F. 2013. Development of a "first principles" water potential with flexible monomers: dimer potential energy surface, VRT spectrum, and second virial coefficient. *J. Chem. Theory Comput.* 9:5395–403
9. Xie W, Liu L, Sun Z, Guo H, Dawes R. 2015. State-to-state reaction dynamics of $^{18}O+^{32}O_2$ studied by a time-dependent quantum wavepacket method. *J. Chem. Phys.* 142:064308
10. Sun Z, Yu D, Xie W, Hou J, Dawes R, Guo H. 2015. Kinetic isotope effect of the $^{16}O+^{36}O_2$ and $^{18}O+^{32}O_2$ isotope exchange reactions: dominant role of reactive resonances revealed by an accurate time-dependent quantum wavepacket study. *J. Chem. Phys.* 142:174312
11. Rajagopala R, Guillon G, Mahapatra S, Honvault P. 2015. Quantum dynamics of $^{16}O+^{36}O_2$ and $^{18}O+^{32}O_2$ exchange reactions. *J. Chem. Phys.* 142:174311
12. Dawes R, Lolur P, Ma J, Guo H. 2011. Highly accurate ozone formation potential and implications for kinetics. *J. Chem. Phys.* 135:081102
13. Dawes R, Lolur P, Li A, Jiang B, Guo H. 2013. An accurate global potential energy surface for the ground electronic state of ozone. *J. Chem. Phys.* 139:201103
14. Powell A, Dattani N, Spada R, Machado F, Lischka H, Dawes R. 2017. Investigation of the ozone formation reaction pathway: comparisons of FCIQMC and fixed-node diffusion Monte Carlo with contracted and uncontracted MRCI. *J. Chem. Phys.* 147:094306
15. Frost A, Musulin B. 1954. Semiempirical potential energy functions. I. The H_2 and H_2^+ diatomic molecules. *J. Chem. Phys.* 22:1017–20
16. Sato S. 1955. On a new method of drawing the PES. *J. Chem. Phys.* 23:592–93
17. Goodeve CF. 1934. 3D models of the PES of triatomic systems. *Trans. Faraday Soc.* 30:60–68
18. Dye JL. 1957. Model of a potential energy surface. *J. Chem. Educ.* 34:215–16
19. Teller E. 1937. The crossing of potential surfaces. *J. Phys. Chem.* 41:109–16
20. Le Roy RJ, Henderson R. 2007. A new potential function form incorporating extended long-range behaviour: application to ground-state Ca_2. *Mol. Phys.* 105:663–77
21. Szalewicz K. 2012. Symmetry-adapted perturbation theory of intermolecular forces. *Wiley Interdiscip. Rev. Comput. Mol. Sci.* 2:254–72
22. Jansen G. 2014. Symmetry-adapted perturbation theory based on density functional theory for noncovalent interactions. *Wiley Interdiscip. Rev. Comput. Mol. Sci.* 4:127–44
23. McDaniel JG, Schmidt JR. 2013. Physically-motivated force fields from symmetry-adapted perturbation theory. *J. Phys. Chem. A* 117:2053–66
24. Xie C, Zhao B, Malbon C, Yarkony DR, Xie D, Guo H. 2019. Insights into the mechanism of nonadiabatic photodissociation from product vibrational distributions. The remarkable case of phenol. *J. Phys. Chem. Lett.* 11:191–98

25. Describes fitting three electronic states of phenol in 33 dimensions.

25. **Zhu X, Yarkony DR. 2014. Fitting coupled PESs for large systems: method and construction of a 3-state representation for phenol photodissociation in the full 33 internal degrees of freedom using multireference configuration interaction determined data. *J. Chem. Phys.* 140:24112**
26. Werner H, Knowles P, Manby F, Black J, Doll K, et al. 2020. The MolPro quantum chemistry package. *J. Chem. Phys.* 152:144107
27. Frisch M, Trucks G, Schlegel H, Scuseria G, Robb M, et al. 2016. Gaussian 16, revis. C.01. *Software Package*. **https://gaussian.com/relnotes/**

28. Stanton J, Gauss J, Harding M, Szalay P, Auer A, et al. 2009. CFOUR. *Software Package*. **http://www.cfour.de**
29. Krylov A, Gill P. 2013. Q-Chem: an engine for innovation. *Wiley Interdiscip. Rev. Comput. Mol. Sci.* 3:317–26
30. Kállay M, Nagy P, Mester D, Rolik Z, Samu G, et al. 2020. The MRCC program system: accurate quantum chemistry from water to proteins. *J. Chem. Phys.* 152:074107
31. Lischka H, Shepard R, Pitzer R, Shavitt I, Dallos M, et al. 2001. High-level multireference methods in the quantum-chemistry program system COLUMBUS: analytic MR-CISD and MR-AQCC gradients and MR-AQCC-LRT for excited states, GUGA spin–orbit CI and parallel CI density. *Phys. Chem. Chem. Phys.* 3:664–67
32. Van Dam H, De Jong W, Bylaska E, Govind N, Kowalski K, et al. 2011. NWChem: scalable parallel computational chemistry. *Wiley Interdiscip. Rev. Comput. Mol. Sci.* 1:888–94
33. Dawes R, Ndengué SA. 2016. Single- and multireference electronic structure calculations for constructing potential energy surfaces. *Int. Rev. Phys. Chem.* 35:441–78
34. Smith D, Jankowski P, Slawik M, Witek H, Patkowski K. 2014. Basis set convergence of the post-CCSD(T) contribution to noncovalent interaction energies. *J. Chem. Theory Comput.* 10:3140–50
35. Murphy K, Schaefer H, Agarwal J. 2017. Phosgene at the complete basis set limit of CCSDT(Q): molecular structure and rovibrational analysis. *Chem. Phys. Lett.* 683:12–17
36. Demovičová L, Hobza P, Řezáč J. 2014. Evaluation of composite schemes for CCSDT(Q) calculations of interaction energies of noncovalent complexes. *Phys. Chem. Chem. Phys.* 16:19115–21
37. Matthews D, Stanton J. 2015. Non-orthogonal spin-adaptation of coupled cluster methods: a new implementation of methods including quadruple excitations. *J. Chem. Phys.* 142:064108
38. Kats D, Köhn A. 2019. On the distinguishable cluster approximation for triple excitations. *J. Chem. Phys.* 150:151101
39. Parrish R, Zhao Y, Hohenstein E, Martínez TJ. 2019. Rank reduced coupled cluster theory. I. Ground state energies and wavefunctions. *J. Chem. Phys.* 150:164118
40. Rolik Z, Kállay M. 2011. Cost reduction of high-order coupled-cluster methods via active-space and orbital transformation techniques. *J. Chem. Phys.* 134:124111
41. Rolik Z, Kállay M. 2018. Novel strategy to implement active-space coupled-cluster methods. *J. Chem. Phys.* 148:124108
42. Ndengué S, Dawes R, Guo H. 2016. A new set of PESs for HCO: influence of Renner–Teller coupling on the bound and resonance vibrational states. *J. Chem. Phys.* 144:244301
43. Davidson ER, Silver DW. 1977. Size consistency in the dilute helium gas electronic structure. *Chem. Phys. Lett.* 52:403–6
44. Piecuch P, Oliphant N, Adamowicz L. 1993. A state-selective multireference coupled-cluster theory employing the single-reference formalism. *J. Chem. Phys.* 99:1875–1900
45. Hanauer M, Köhn A. 2012. Perturbative treatment of triple excitations in internally contracted multireference coupled cluster theory. *J. Chem. Phys.* 136:204107
46. Evangelista F. 2018. Multireference coupled cluster theories of dynamical electron correlation. *J. Chem. Phys.* 149:030901
47. Magoulas I, Bauman N, Shen J, Piecuch P. 2018. Application of the CC(P;Q) hierarchy of coupled-cluster methods to the beryllium dimer. *J. Phys. Chem. A* 122:1350–68
48. Deustua JE, Yuwono S, Shen J, Piecuch P. 2019. Accurate excited-state energetics by a combination of Monte Carlo sampling and equation-of-motion coupled-cluster computations. *J. Chem. Phys.* 150:111101
49. Blunt N, Neuscamman E. 2018. Excited-state diffusion Monte Carlo calculations: a simple and efficient two-determinant ansatz. *J. Chem. Theory Comput.* 15:178–89
50. Zgid D, Nooijen M. 2008. On the spin and symmetry adaptation of the density matrix renormalization group method. *J. Chem. Phys.* 128:014107
51. Yanai T, Kurashige Y, Neuscamman E, Chan G. 2010. Multireference quantum chemistry through a joint density matrix renormalization group and canonical transformation theory. *J. Chem. Phys.* 132:024105

33. Presents detailed recommendations for developing electronic structure protocols.

52. Phillips J, Zgid D. 2014. The description of strong correlation within self-consistent Green's function second-order perturbation theory. *J. Chem. Phys.* 140:241101
53. Neuhauser D, Baer R, Zgid D. 2017. Stochastic self-consistent 2nd-order Gree's function method for correlation energies of large systems. *J. Chem. Theory Comput.* 13:5396–403
54. Stanton S, Bartlett R. 1993. The equation of motion coupled-cluster method. A systematic biorthogonal approach to molecular excitation energies, transition probabilities, and excited state properties. *J. Chem. Phys.* 98:7029–39
55. Krylov A. 2008. Equation-of-motion coupled-cluster methods for open-shell and electronically excited species: the hitchhiker's guide to Fock space. *Annu. Rev. Phys. Chem.* 59:433–62
56. Hill JG, Peterson KA, Knizia G, Werner H-J. 2009. Extrapolating MP2 and CCSD explicitly correlated correlation energies to the complete basis set limit with first and second row correlation consistent basis sets. *J. Chem. Phys.* 131:194105
57. Feller D, Peterson K. 2013. An expanded calibration study of the explicitly correlated CCSD(T)-F12b method using large basis set standard CCSD(T) atomization energies. *J. Chem. Phys.* 139:084110
58. Sylvetsky N, Peterson K, Karton A, Martin J. 2016. Toward a W4-F12 approach: Can explicitly correlated and orbital-based ab initio CCSD(T) limits be reconciled? *J. Chem. Phys.* 144:214101
59. Harding M, Vázquez J, Ruscic B, Wilson A, Gauss J, Stanton J. 2008. High-accuracy extrapolated ab initio thermochemistry. III. Additional improvements and overview. *J. Chem. Phys.* 128:114111
60. Ganyecz Á, Kállay M, Csontos J. 2017. Moderate-cost ab initio thermochemistry with chemical accuracy. *J. Chem. Theory Comput.* 13:4193–204
61. Le Roy R, Huang Y, Jary C. 2006. An accurate analytic potential function for ground-state N_2 from a direct-potential-fit analysis of spectroscopic data. *J. Chem. Phys.* 125:164310
62. Le Roy R, Haugen CC, Tao J, Li H. 2011. Long-range damping functions improve the short-range behaviour of 'MLR' potential energy functions. *Mol. Phys.* 109:435–46
63. Li H, Le Roy R. 2008. Analytic three-dimensional MLR potential energy surface for CO_2-He, and its predicted microwave and infrared spectra. *Phys. Chem. Chem. Phys.* 10:4128–37
64. Stone AJ. 2013. *The Theory of Intermolecular Forces*. Oxford, UK: Oxford Univ. Press
65. Stone AJ. 2005. Distributed multipole analysis: stability for large basis sets. *J. Chem. Theory Comput.* 1:1128–32
66. Hapka M, Zuchowski P, Szcześniak M, Chałasiński G. 2012. Symmetry-adapted perturbation theory based on unrestricted Kohn–Sham orbitals for high-spin open-shell van der Waals complexes. *J. Chem. Phys.* 137:164104
67. Garcia J, Podeszwa R, Szalewicz K. 2020. SAPT codes for calculations of intermolecular interaction energies. *J. Chem. Phys.* 152:184109
68. Xu C, Jiang B, Xie D, Farantos S, Lin S, Guo H. 2007. Analysis of the HO_2 vibrational spectrum on an accurate ab initio potential energy surface. *J. Phys. Chem. A* 111:10353–61
69. Ishida T, Schatz G. 1999. A local interpolation scheme using no derivatives in quantum-chemical calculations. *Chem. Phys. Lett.* 314:369–75
70. Maisuradze G, Thompson D. 2003. Interpolating moving least-squares methods for fitting potential energy surfaces: illustrative approaches and applications. *J. Phys. Chem. A* 107:7118–24
71. Dawes R, Thompson D, Guo Y, Wagner A, Minkoff M. 2007. Interpolating moving least-squares methods for fitting potential energy surfaces: computing high-density potential energy surface data from low-density ab initio data points. *J. Chem. Phys.* 126:184108
72. Ischtwan J, Collins M. 1994. Molecular PESs by interpolation. *J. Chem. Phys.* 100:8080–88
73. Ho TS, Rabitz H. 2003. Reproducing kernel Hilbert space interpolation methods as a paradigm of HDMR: application to multidimensional PES construction. *J. Chem. Phys.* 119:6433–42
74. Christianen A, Karman T, Vargas-Hernández R, Groenenboom G, Krems R. 2019. Six-dimensional potential energy surface for NaK–NaK collisions: Gaussian process representation with correct asymptotic form. *J. Chem. Phys.* 150:064106
75. Uteva E, Graham R, Wilkinson R, Wheatley R. 2018. Active learning in Gaussian process interpolation of potential energy surfaces. *J. Chem. Phys.* 149:174114

76. Nguyen T, Székely E, Imbalzano G, Behler J, Csányi G, et al. 2018. Comparison of PIPs, neural networks, and Gaussian approximation potentials in representing water interactions through many-body expansions. *J. Chem. Phys.* 148:241725
77. Manzhos S, Wang X-G, Dawes R, Carrington T. 2006. A nested molecule-independent neural network approach for high-quality potential fits. *J. Phys. Chem. A* 110:5295–304
78. Manzhos S, Dawes R, Carrington T Jr. 2015. Neural network-based approaches for building high dimensional and quantum dynamics–friendly PESs. *Int. J. Quantum Chem.* 115:1012–20
79. Brown A, Pradhan E. 2017. Fitting potential energy surfaces to sum-of-products form with neural networks using exponential neurons. *J. Theor. Comput. Chem.* 16:1730001
80. Dral PO, Owens A, Yurchenko SN, Thiel W. 2017. Structure-based sampling and self-correcting machine learning for accurate calculations of potential energy surfaces and vibrational levels. *J. Chem. Phys.* 146:244108
81. Qu C, Yu Q, Bowman J. 2018. Permutationally invariant potential energy surfaces. *Annu. Rev. Phys. Chem.* 69:151–75
82. Li J, Jiang B, Guo H. 2013. Permutation invariant polynomial neural network approach to fitting potential energy surfaces. II. Four-atom systems. *J. Chem. Phys.* 139:204103
83. Shao K, Chen J, Zhao Z, Zhang D. 2016. Fitting potential energy surfaces with fundamental invariant neural network. *J. Chem. Phys.* 145:071101
84. Bender J, Doraiswamy S, Truhlar D, Candler G. 2014. Potential energy surface fitting by a statistically localized, permutationally invariant, local interpolating moving least squares method for the many-body potential: method and application to N_4. *J. Chem. Phys.* 140:054302
85. Majumder M, Hegger SE, Dawes R, Manzhos S, Wang XG, Carrington T Jr. 2015. Explicitly correlated MRCI-F12 potential energy surfaces for methane fit with several permutation invariant schemes and full-dimensional vibrational calculations. *Mol. Phys.* 113:1823–33
86. Noé F, Tkatchenko A, Müller K-R, Clementi C. 2020. Machine learning for molecular simulation. *Annu. Rev. Phys. Chem.* 71:361–90
87. Abbott A, Turney J, Zhang B, Smith D, Altarawy D, Schaefer H III. 2019. PES-Learn: an open-source software package for the automated generation of machine learning models of molecular potential energy surfaces. *J. Chem. Theory Comput.* 15:4386–98
88. Dawes R, Quintas-Sánchez E. 2018. The construction of ab initio–based potential energy surfaces. In *Reviews in Computational Chemistry*, Vol. 31, ed. AL Parrill, KB Lipkowitz, pp. 199–263. Hoboken, NJ: John Wiley & Sons
89. Kamath A, Vargas-Hernández R, Krems R, Carrington T Jr., Manzhos S. 2018. Neural networks versus Gaussian process regression for representing potential energy surfaces: a comparative study of fit quality and vibrational spectrum accuracy. *J. Chem. Phys.* 148:241702
90. Dawes R, Wagner A, Thompson D. 2009. Ab initio wavenumber accurate spectroscopy: $^1CH_2$ and HCN vibrational levels on automatically generated IMLS potential energy surfaces. *J. Phys. Chem. A* 113:4709–21
91. Dawes R, Wang X-G, Jasper A, Carrington T Jr. 2010. Nitrous oxide dimer: a new potential energy surface and rovibrational spectrum of the nonpolar isomer. *J. Chem. Phys.* 133:134304
92. Brown J, Wang X-G, Carrington T Jr., Grubbs GS, Dawes R. 2014. Computational study of the rovibrational spectrum of CO_2–CS_2. *J. Chem. Phys.* 140:114303
93. Pandey A, Poirier B. 2020. An algorithm to find (and plug) "holes" in multi-dimensional surfaces. *J. Chem. Phys.* 152:214102
94. Quintas-Sánchez E, Dawes R. 2019. AUTOSURF: a freely available program to construct potential energy surfaces. *J. Chem. Inf. Model.* 59:262–71
95. Metz M, Szalewicz K, Sarka J, Tóbiás R, Császár A, Mátyus E. 2019. Molecular dimers of methane clathrates: ab initio potential energy surfaces and variational vibrational states. *Phys. Chem. Chem. Phys.* 21:13504–25
96. Győri T, Czako G. 2019. Automating the development of high-dimensional reactive potential energy surfaces with the ROBOSURFER program system. *J. Chem. Theory Comput.* 16:51–66
97. Brown J, Wang X-G, Dawes R, Carrington T Jr. 2012. Computational study of the rovibrational spectrum of $(OCS)_2$. *J. Chem. Phys.* 136:134306

98. Wang X-G, Carrington T Jr., Dawes R. 2016. Computational study of the rovibrational spectrum of $(CO2)_2$. *J. Mol. Spectrosc.* 330:179–87
99. Donoghue G, Wang X-G, Dawes R, Carrington T Jr. 2016. Computational study of the rovibrational spectra of CO_2–C_2H_2 and CO_2–C_2D_2. *J. Mol. Spectrosc.* 330:170–78
100. Dawes R, Wang X-G, Carrington T Jr. 2013. CO dimer: new potential energy surface and rovibrational calculations. *J. Phys. Chem. A* 117:7612–30
101. Walker K, Dumouchel F, Lique F, Dawes R. 2016. The first PESs for the C_6H–H_2 and C_6H–He collisional systems and their corresponding inelastic cross sections. *J. Chem. Phys.* 145:024314
102. Barton EJ, Yurchenko SN, Tennyson J, Clausen S, Fateev A. 2015. High-resolution absorption measurements of NH_3 at high temperatures: 500–2100 cm^{-1}. *J. Quant. Spectrosc. Radiat. Transf.* 167:126–34
103. Barton EJ, Polyansky OL, Yurchenko SN, Tennyson J, Civiš S, et al. 2017. Absorption spectra of ammonia near 1 μm. *J. Quant. Spectrosc. Radiat. Transf.* 203:392–97
104. Barton EJ, Yurchenko SN, Tennyson J, Clausen S, Fateev A. 2017. High-resolution absorption measurements of NH_3 at high temperatures: 2100–5500 cm^{-1}. *J. Quant. Spectrosc. Radiat. Transf.* 189:60–65

105. HITRAN is an extensive spectroscopic database combining data from both theoretical predictions and experimental measurements.

105. Gordon IE, Rothman L, Hill C, Kochanov R, Tan Y, et al. 2017. The HITRAN2016 molecular spectroscopic database. *J. Quant. Spectrosc. Radiat. Transf.* 203:3–69

106. Ayouz M, Babikov D. 2013. Global permutationally invariant potential energy surface for ozone forming reaction. *J. Chem. Phys.* 138:164311
107. Mikhailenko S, Barbe A. 2020. High resolution infrared spectrum of $^{16}O_3$: the 3600–4300 cm^{-1} range reinvestigated. *J. Quant. Spectrosc. Radiat. Transf.* 244:106823
108. Coles P, Yurchenko S, Tennyson J. 2019. ExoMol molecular line lists. XXXV. A rotation-vibration line list for hot ammonia. *Mon. Not. R. Astron. Soc.* 490:4638–47
109. Darby-Lewis D, Shah H, Joshi D, Khan F, Kauwo M, et al. 2019. MARVEL analysis of the measured high-resolution spectra of ^{14}NH. *J. Mol. Spectrosc.* 362:69–76
110. Furtenbacher T, Coles P, Tennyson J, Yurchenko SN, Yu S, et al. 2020. Empirical rovibrational energy levels of ammonia up to 7500 cm^{-1}. *J. Quant. Spectrosc. Radiat. Transf.* 251:107027
111. Ndengué S, Dawes R, Wang X-G, Carrington T Jr., Sun Z, Guo H. 2016. Calculated vibrational states of ozone up to dissociation. *J. Chem. Phys.* 144:074302
112. Wang X-G, Carrington T Jr. 2020. A variational calculation of vibrational levels of vinyl radical. *J. Chem. Phys.* 152:204311
113. Yu H-G. 2016. An exact variational method to calculate rovibrational spectra of polyatomic molecules with large amplitude motion. *J. Chem. Phys.* 145:084109
114. Zhao Z, Chen J, Zhang Z, Zhang DH, Lauvergnat D, Gatti F. 2016. Full-dimensional vibrational calculations of five-atom molecules using a combination of Radau and Jacobi coordinates: applications to methane and fluoromethane. *J. Chem. Phys.* 144:204302
115. Carrington T Jr. 2017. Computing (ro-)vibrational spectra of molecules with more than four atoms. *J. Chem. Phys.* 146:120902
116. Yurchenko S, Yachmenev A, Ovsyannikov R. 2017. Symmetry-adapted ro-vibrational basis functions for variational nuclear motion calculations: TROVE approach. *J. Chem. Theory Comput.* 13:4368–81
117. Pandey A, Poirier B. 2019. Using phase-space Gaussians to compute the vibrational states of $OCHCO^+$. *J. Chem. Phys.* 151:014114
118. Avila G, Mátyus E. 2019. Toward breaking the curse of dimensionality in (ro)vibrational computations of molecular systems with multiple large-amplitude motions. *J. Chem. Phys.* 150:174107
119. Avila G, Matyus E. 2019. Full-dimensional (12D) variational vibrational states of $CH_4{\cdot}F^-$: interplay of anharmonicity and tunneling. *J. Chem. Phys.* 151:154301
120. Rey M, Nikitin A, Campargue A, Kassi S, Mondelain D, Tyuterev V. 2016. Ab initio variational predictions for understanding highly congested spectra: rovibrational assignment of 108 new methane subbands in the icosad range. *Phys. Chem. Chem. Phys.* 18:176–89
121. Kumar P, Poirier B. 2019. The J-dependent rotational Hamiltonian method for analyzing rovibrational spectra: application to HO_2, H_2O, and O_3. *Chem. Phys. Lett.* 733:136700
122. Csaszar A, Furtenbacher T, Arendas P. 2016. Small molecules and big data. *J. Phys. Chem. A* 120:8949–69
123. Castro-Juárez E, Wang X-G, Carrington T Jr., Quintas-Sánchez E, Dawes R. 2019. Computational study of the ro-vibrational spectrum of CO–CO_2. *J. Chem. Phys.* 151:084307

124. Cybulski H, Henriksen C, Dawes R, Wang X-G, Bora N, et al. 2018. Ab initio study of the CO–N_2 complex: a new highly accurate intermolecular potential energy surface and rovibrational spectrum. *Phys. Chem. Chem. Phys.* 20:12624–36
125. Walker KM, Lique F, Dawes R. 2018. Fine and hyperfine collisional excitation of C_6H by He. *Mon. Not. R. Astron. Soc.* 473:1407–15
126. Barclay AJ, McKellar ARW, Moazzen-Ahmadi N, Dawes R, Wang X-G, Carrington T Jr. 2018. Infrared spectrum and intermolecular potential energy surface of the CO–O_2 dimer. *Phys. Chem. Chem. Phys.* 20:14431–40
127. Sur S, Quintas-Sánchez E, Ndengué S, Dawes R. 2019. Development of a PES for the O_3–Ar system: rovibrational states of the complex. *Phys. Chem. Chem. Phys.* 21:9168–80
128. Quintas-Sánchez E, Dawes R, Lee K, McCarthy M. 2020. Automated construction of potential energy surfaces suitable to describe van der Waals complexes with highly-excited nascent molecules: the rotational spectra of Ar–CS(v) and Ar–SiS(v). *J. Phys. Chem. A* 124:4445–54
129. Levine R. 2009. *Molecular Reaction Dynamics*. Cambridge, UK: Cambridge Univ. Press
130. Brouard M, Chadwick H, Eyles CJ, Aoiz FJ, Kłos J. 2011. The *k-j-j′* vector correlation in inelastic and reactive scattering. *J. Chem. Phys.* 135:084305
131. Truhlar D, Wyatt R. 1977. H + H_2: potential-energy surfaces and elastic and inelastic scattering. In *Advances in Chemical Physics*, Vol. 36, ed. I Prigogine, SA Rice, pp. 141–204. New York: John Wiley & Sons
132. Zhou B, Yang B, Balakrishnan N, Kendrick B, Stancil P. 2020. Prediction of a Feshbach resonance in the below-the-barrier reactive scattering of vibrational excited HD with H. *J. Phys. Chem. Lett.* 11:4970–75
133. Neumark D, Wodtke A, Robinson G, Hayden C, Lee Y. 1985. Molecular beam studies of the F+H_2 reaction. *J. Chem. Phys.* 82:3045–66
134. Alexander M, Werner H-J, Manolopoulos D. 1998. Spin-orbit effects in the reaction of F(^{2}P) with H_2. *J. Chem. Phys.* 109:5710–13
135. Qiu M, Ren Z, Che L, Dai D, Harich S, et al. 2006. Observation of Feshbach resonances in the F+H_2→HF+H reaction. *Science* 311:1440–43
136. Fu B, Shan X, Zhang D, Clary DC. 2017. Recent advances in quantum scattering calculations on polyatomic bimolecular reactions. *Chem. Soc. Rev.* 46:7625–49
137. Maiti B, Schatz G. 2003. Theoretical studies of intersystem crossing effects in the O(^{3}P, ^{1}D)+H_2 reaction. *J. Chem. Phys.* 119:12360–71
138. Lendvay G, Schatz G. 2019. Quantum scattering theory for collisional energy transfer. *Comp. Chem. Kinet.* 43:63–107
139. Ndengué S, Dawes R, Gatti F, Meyer H. 2017. Atom-triatom rigid rotor inelastic scattering with the multiconfiguration time dependent Hartree approach. *Chem. Phys. Lett.* 668:42–46
140. Ndengué S, Scribano Y, Gatti F, Dawes R. 2019. State-to-state inelastic rotational cross sections in five-atom systems with the MCTDH method. *J. Chem. Phys.* 151:134301
141. Sur S, Ndengué S, Quintas-Sánchez E, Bop B, Lique F, Dawes R. 2020. Rotationally inelastic scattering of O_3-Ar: state-to-state rates with the multiconfigurational time dependent Hartree method. *Phys. Chem. Chem. Phys.* 22:1869–80
142. Babikov D, Semenov A. 2016. Recent advances in development and applications of the mixed quantum/classical theory for inelastic scattering. *J. Phys. Chem. A* 120:319–31
143. Desrousseaux B, Quintas-Sánchez E, Dawes R, Lique F. 2019. Collisional excitation of CF^+ by H_2: potential energy surface and rotational cross sections. *J. Phys. Chem. A* 123:9637–43
144. Faure A, Dagdigian P, Rist C, Dawes R, Quintas-Sánchez E, et al. 2019. Interaction of chiral propylene oxide (CH_3CHCH_2O) with helium: potential energy surface and scattering calculations. *ACS Earth Space Chem.* 3:964–72
145. Bop B, Batista-Romero F, Faure A, Quintas-Sánchez E, Dawes R, Lique F. 2019. Isomerism effects in the collisional excitation of cyanoacetylene by molecular hydrogen. *ACS Earth Space Chem.* 3:1151–57
146. Plomp V, Gao Z, Cremers T, Besemer M, van de Meerakker S. 2020. High-resolution imaging of molecular collisions using a Zeeman decelerator. *J. Chem. Phys.* 152:091103

129. Presents a thought-provoking, in-depth treatment of gas-phase reaction dynamics.